Numerical valuation of two-asset options under jump diffusion models using Gauss-Hermite quadrature

M. Fakharany[a], V. N. Egorova[b,c,1], R. Company[b]

[a] *Mathematics Department, Faculty of Science, Tanta University. Tanta-Egypt.*
[b] *Instituto de Matemática Multidisciplinar, Universitat Politècnica de València, Camino de Vera s/n, 46022 Valencia, Spain.*
[c] *BCAM, Basque Center for Applied Mathematics, Mazarredo 14, E48009 Bilbao, Basque Country, Spain.*

Abstract

In this work a finite difference approach together with a bivariate Gauss-Hermite quadrature technique are developed for partial-integro differential equations related to option pricing problems on two underlying asset driven by jump-diffusion models. Firstly, the mixed derivative term is removed using a suitable transformation avoiding numerical drawbacks such as slow convergence and inaccuracy due to the appearance of spurious oscillations. Unlike the more traditional truncation approach we use 2D Gauss-Hermite quadrature with the additional advantage of saving computational cost. The explicit finite difference scheme becomes consistent, conditionally stable and positive. European and American option cases are treated. Numerical results are illustrated and analyzed with experiments and comparisons with other well recognized methods.

Keywords: Two-asset option pricing, partial-integro differential equation, jump-diffusion models, numerical analysis, bivariate Gauss-Hermite quadrature.

Email addresses: fakharany@aucegypt.edu (M. Fakharany), egorova.vn@gmail.com (V. N. Egorova), rcompany@imm.upv.es (R. Company)
[1] corresponding author

1. Introduction

It is well known that Black-Scholes model does not capture stock price fluctuations and market risks, for instance, features like heavy tails and asymmetries observed in market-data log returns densities [1]. Jump diffusion models is a class of alternative ones to improve the lack of jumps in the asset prices which are natural for instance when they appear earning surprises or other types of discrete economic events [2]. With respect to the mathematical formulation of the option price valuation the main difference is the appearance of an integral term achieving a partial integro-differential equation (PIDE) instead of a partial differential equation (PDE). The jumps in the logarithm of the prices may be distributed by any finite activity process and depending on it the integral in the PIDE problem has a different kernel [2, 3, 4]. An overview of different methods for solving one asset option pricing jump diffusion models may be found in the introduction of [5].

Two asset American claims under jump diffusion have been priced using a Markov chain approach that can be essentially regarded as an explicit finite difference method in [6]. The jump terms managed in [6] may be regarded as un extension of the method in [7]. An implicit finite difference method for two asset jump diffusion option pricing models has been proposed in [5]. The appearance of dense linear systems in the discretization of the integral part of the underlying PIDE is avoided by combining a fixed point iteration scheme with a Fast Fourier Transform (FFT). The new two asset technique developed in [5] is able to price options with general types of payoffs and barriers for European as well as American options.

More recently the authors in [8] employ high-order Galerkin finite element discretizations for both two asset option pricing problems and stochastic volatility models. The resulting semi-discrete systems are solved using exponential time integration. Difficulties arising in the treatment of two asset jump diffusion PIDE models are similar to those of one asset stochastic volatility jump diffusion problems. Both two dimensional PIDE problems involve a non local

integral term together with the corresponding differential part including a cross derivative term linked to the correlation between the variables [9, 10].

This paper deals with two dimensional Merton jump diffusion model where the stochastic differential equations for the underlying assets changes are given by

$$\frac{dS_i(t)}{S_i(t)} = (r - q_i - \lambda\kappa_i)dt + \sigma_i dW_i + (e^{J_i} - 1)dZ(t), \quad i = 1, 2, \tag{1}$$

where S_i, q_i, σ_i, $i = 1, 2$ are the two assets prices, asset dividend yields, asset volatilities respectively, r is the risk free interest and W_i are standard Brownian motions correlated by $\rho \in (-1, 1)$. Here J_1 and J_2 are the jump sizes correlated by $\rho_J \in (-1, 1)$, κ_i represent the expected relative jump sizes ($\kappa_i = \mathbb{E}[e^{J_i} - 1]$), Z and λ are the Poisson process and its jump intensity [8]. Based on Itô calculus, the corresponding PIDE for the unknown option price $U(x_1, x_2, \tau)$ takes the form

$$\begin{aligned}\frac{\partial U}{\partial \tau} =& \frac{\sigma_1^2}{2}\frac{\partial^2 U}{\partial x_1^2} + \rho\sigma_1\sigma_2\frac{\partial^2 U}{\partial x_1 \partial x_2} + \frac{\sigma_2^2}{2}\frac{\partial^2 U}{\partial x_2^2} + \left(r - q_1 - \lambda\kappa_1 - \frac{\sigma_1^2}{2}\right)\frac{\partial U}{\partial x_1} \\ &+ \left(r - q_2 - \lambda\kappa_2 - \frac{\sigma_2^2}{2}\right)\frac{\partial U}{\partial x_2} - (r + \lambda)U \\ &+ \lambda \int_{\mathbb{R}^2} U(x_1 + \eta_1, x_2 + \eta_2) g(\eta_1, \eta_2) d\eta_1 d\eta_2,\end{aligned} \tag{2}$$

where $(x_1, x_2) = (\ln(S_1/E), \ln(S_2/E))$, E is the strike price, $\tau = T - t$ is the time to maturity and $g(\eta_1, \eta_2)$ is the probability density function of a bivariate normal distribution, given by

$$g(\eta_1, \eta_2) = \frac{\exp\left[-\frac{1}{2(1-\rho_J^2)}\left(\left(\frac{\eta_1 - \mu_1}{\hat{\sigma}_1}\right)^2 - \frac{2\rho_J(\eta_1 - \mu_1)(\eta_2 - \mu_2)}{\hat{\sigma}_1\hat{\sigma}_2} + \left(\frac{\eta_2 - \mu_2}{\hat{\sigma}_2}\right)^2\right)\right]}{2\pi\hat{\sigma}_1\hat{\sigma}_2\sqrt{1 - \rho_J^2}}, \tag{3}$$

such that μ_1, μ_2, $\hat{\sigma}_1$ and $\hat{\sigma}_2$ are the means and standard deviations of the jumps J_1 and J_2 respectively [5, 8]. There are several kinds of two asset problems depending on the nature of the payoff. Here the option gives a holder the right to receive the maximum or minimum of the two underlying assets at maturity. The payoff $f(x_1, x_2)$ for put on the minimum of two asset [5, 12] and the boundary

conditions are given by

$$
\begin{aligned}
&f(x_1, x_2) = E \max(1 - \min(e^{x_1}, e^{x_2}), 0), \\
&\lim_{x_1 \to -\infty} U(x_1, x_2, \tau) = E e^{-r\tau}, \quad \lim_{x_2 \to -\infty} U(x_1, x_2, \tau) = E e^{-r\tau}, \\
&U(x_1, x_2, \tau) \approx f(x_1, x_2), \text{ as } x_1 \to \infty \text{ or } x_2 \to \infty.
\end{aligned} \tag{4}
$$

The cross derivative term in the differential part of the PIDE problem may involves unsuitable effects in the computations throughout finite difference schemes due to the appearance of negative coefficient terms in the approximation of the derivative as well as in the cost of the points stencil schemes. Both facts favor potential drawbacks arising from the dominance of the convection versus the diffusion terms [10, 11, 14]. In order to avoid these numerical drawbacks it is convenient to transform the original PIDE problem (2) into another one where the cross derivative one disappears. This technique has been successfully developed in [14, 15]. Another strategy to reduce the number of points in the stencil schemes is based on special approximation of the mixed derivative, see [9, 10].

With respect to the numerical treatment of the integral part of the PIDE problem we use a different approach of those developed in [5] and [8]. In fact, we use two dimensional Gauss-Hermite quadrature that has the advantage of obtaining accurate approximations with a very reduced number of quadrature nodes that do not need to be mesh points of our numerical domain. Then a bivariate interpolation is needed to approximate the integral part of the PIDE. One dimensional Gauss-Hermite quadrature has been used for one asset option pricing problems in [9] and Gauss-Laguerre quadrature in [16].

This paper is organized as follows. In Section 2, the mixed derivative is removed using suitable transformation after an adimensional transformation. Discretization of the transformed problem is addressed in Section 3. Numerical analysis issues including positivity, stability and consistency are treated in Sections 4 and 5. The proposed scheme is extended to cover the American option case in Section 6. Section 7 includes numerical examples illustrating efficient performance of the proposed numerical scheme.

Let us recall some definitions and notations that will be used along the paper. Given a vector $\mathbf{u} \in \mathbb{R}^n$ such that $\mathbf{u} = (u_1, u_2, \ldots, u_n)^T$, the infinite norm of $\mathbf{u}$ is denoted by $\|\mathbf{u}\|_\infty$ and is defined as $\|\mathbf{u}\|_\infty = \max\{u_j,\ 1 \leq j \leq n\}$. The vector $\mathbf{u}$ is said to be nonnegative if $u_j \geq 0$ for all $1 \leq j \leq n$, and it is denoted by $\mathbf{u} \geq 0$. For a matrix $B = (b_{ij})_{m\times n}$ in $\mathbb{R}^{m\times n}$, its infinite norm is given by $\|B\|_\infty = \max_{1\leq i\leq m}\{\sum_{j=1}^n |b_{ij}|\}$. Thus, if A is a block matrix with $m \times n$ block entries A_{ij}, then the infinite norm of A is given by, see [13, Chap. 2],

$$\|A\|_\infty = \max_{1\leq i\leq m} \{\|[A_{i1}\ A_{i2} \ldots A_{in}]\|_\infty\}. \tag{5}$$

Matrix A is said to be nonnegative if $a_{ij} \geq 0$ for all $1 \leq i \leq m$, $1 \leq j \leq n$, and we denote $A \geq 0$.

2. Uncorrelating transformation

Let us begin this section with the dimensionless transformation of (2)-(4) given by the substitutions

$$\bar{\tau} = \frac{\tau}{T}, \quad \bar{U} = \frac{U}{E}. \tag{6}$$

Also, the non-dimensional coefficients $\bar{r}$, $\bar{q}_i$, $\bar{\sigma}_i$, $i = 1, 2$ and $\bar{\lambda}$ are given by

$$\bar{r} = rT,\ \bar{q}_i = q_i T,\ \bar{\sigma}_i = \sigma_i\sqrt{T},\ i = 1, 2;\ \bar{\lambda} = \lambda T. \tag{7}$$

Hence equation (2) takes the form

$$\begin{aligned}\frac{\partial \bar{U}}{\partial \bar{\tau}} =& \frac{\bar{\sigma}_1^2}{2}\frac{\partial^2 \bar{U}}{\partial x_1^2} + \rho\bar{\sigma}_1\bar{\sigma}_2\frac{\partial^2 \bar{U}}{\partial x_1 \partial x_2} + \frac{\bar{\sigma}_2^2}{2}\frac{\partial^2 \bar{U}}{\partial x_2^2} + \left(\bar{r} - \bar{q}_1 - \bar{\lambda}\kappa_1 - \frac{\bar{\sigma}_1^2}{2}\right)\frac{\partial \bar{U}}{\partial x_1} \\ &+ \left(\bar{r} - \bar{q}_2 - \bar{\lambda}\kappa_2 - \frac{\bar{\sigma}_2^2}{2}\right)\frac{\partial \bar{U}}{\partial x_2} - (\bar{r} + \bar{\lambda})\bar{U} \\ &+ \bar{\lambda}\int_{\mathbb{R}^2} \bar{U}(x_1 + \eta_1, x_2 + \eta_2)g(\eta_1, \eta_2)d\eta_1 d\eta_2,\end{aligned} \tag{8}$$

and its initial and boundary conditions are given by

$$\begin{aligned}&\bar{f}(x_1, x_2) = \max(1 - \min(e^{x_1}, e^{x_2}), 0), \\ &\lim_{x_1\to-\infty} \bar{U}(x_1, x_2, \bar{\tau}) = e^{-\bar{r}\bar{\tau}},\ \lim_{x_2\to-\infty} \bar{U}(x_1, x_2, \bar{\tau}) = e^{-\bar{r}\bar{\tau}}, \\ &\bar{U}(x_1, x_2, \bar{\tau}) \approx f(x_1, x_2),\ \text{as } x_1 \to \infty \text{ or } x_2 \to \infty.\end{aligned} \tag{9}$$

For simplicity, we write the coefficients and variables without bar. But they still represent the dimensionless form of equations (2) and (4).

Now in order to remove the cross-derivative term, let us consider the canonical transformation based on the characteristic curves technique [17]

$$y_1 = \frac{\sigma_2\tilde{\rho}}{\sigma_1}x_1, \quad y_2 = x_2 - \frac{\sigma_2\rho}{\sigma_1}x_1, \ \tilde{\rho} = \sqrt{1-\rho^2}. \tag{10}$$

In order to remove also the reaction term, let us consider the transformation of the unknown variable

$$V(y_1, y_2, \tau) = \exp((r+\lambda)\tau)U(x_1, x_2, \tau). \tag{11}$$

From (10) and (11), equation (2) becomes

$$\begin{aligned}\frac{\partial V}{\partial \tau} =& \frac{\sigma_2^2\tilde{\rho}^2}{2}\left(\frac{\partial^2 V}{\partial y_1^2} + \frac{\partial^2 V}{\partial y_2^2}\right) + a_1\frac{\partial V}{\partial y_1} + a_2\frac{\partial V}{\partial y_2} \\ &+ \frac{\sigma_1\lambda}{\sigma_2\tilde{\rho}}\int_{\mathbb{R}^2} V(\phi_1, \phi_2, \tau)g(\frac{\sigma_1}{\sigma_2\tilde{\rho}}(\phi_1 - y_1), \phi_2 - y_2 + \tilde{m}(\phi_1 - y_1))d\phi_1 d\phi_2,\end{aligned} \tag{12}$$

where

$$\begin{aligned}a_1 =& \frac{\tilde{\rho}\sigma_2}{\sigma_1}(r - q_1 - \lambda k_1 - \frac{\sigma_1^2}{2}), \\ a_2 =& (1 - \frac{\rho\sigma_2}{\sigma_1})r - (q_2 - \frac{\rho\sigma_2}{\sigma_1}q_1) - \lambda\kappa_2 + \frac{\rho\sigma_2}{\sigma_1}\lambda\kappa_1 - \frac{\sigma_2^2}{2} + \frac{\rho\sigma_1\sigma_2}{2}, \\ \phi_1 =& y_1 + \frac{\sigma_2\tilde{\rho}}{\sigma_1}\eta_1, \ \phi_2 = y_2 - \frac{\sigma_2\rho}{\sigma_1}\eta_1 + \eta_2, \ \tilde{m} = \frac{\rho}{\tilde{\rho}},\end{aligned} \tag{13}$$

and $\phi_1,\ \phi_2$ are the new suitable variables for the integral part with the corresponding Jacobian value $\frac{\sigma_1}{\sigma_2\tilde{\rho}}$.

For the associated boundary conditions (4), one gets

$$\begin{aligned}&\lim_{y_1\to-\infty} V(y_1, y_2, \tau) = e^{\lambda\tau}, \ \lim_{y_2\to-\infty} V(y_1, y_2, \tau) = e^{\lambda\tau}, \\ &V(y_1, y_2, \tau) \approx f(y_1, y_2), \text{ as } y_1 \to \infty \text{ or } y_2 \to \infty.\end{aligned} \tag{14}$$

3. Discretizating

In order to discretize the transformed problem (12), let us choose firstly the bounded numerical domain following criteria of [19, 20]. Thus, let us take a

rectangular domain in x_1x_2- plane with boundaries $x_1 \in [a, b]$ and $x_2 \in [c, d]$ such that e^b and e^d are about ten times the strike E and e^a and e^c are close enough to zero. The values of the endpoints a, b, c and d have an additional condition in order to obtain the Gauss-Hermite quadrature approximation of the integral term. This condition will be explained later. Under the transformation (10), the rectangular domain is converted to a rhomboid domain Ω with vertices $ABCD$ in y_1y_2-plane as shown in Fig.1. Let N_1+1 and N_2+1 be the numbers of mesh points in x_1 and x_2 directions respectively such that the spatial stepsizes are $h_{x_1} = (b-a)/N_1$ and $h_{x_2} = (d-c)/N_2$. From (10) the original mesh points $(N_1 + 1)(N_2 + 1)$ are mapped into the rhomboid domain with new stepsizes $h_1 = \frac{\sigma_2}{\sigma_1}\tilde{\rho}h_{x_1}$, $h_2 = h_{x_2}$. Hence the new rhomboid mesh points are $(y_{1,i}, y^i_{2,j})$ where

$$y_{1,i} = y_{1,0} + ih_1, \quad 0 \le i \le N_1, \quad y_{1,0} = \frac{\sigma_2}{\sigma_1}\tilde{\rho}a, \tag{15}$$

and for each i value,

$$y^i_{2,j} = \hat{y}_{i,0} + jh_2, \quad \hat{y}_{i,0} = c - \frac{\sigma_2}{\sigma_1}\rho(a + ih_{x_1}), \quad 0 \le j \le N_2. \tag{16}$$

The time variable is discretized by $\tau^n = nk$, $0 \le n \le N_\tau$, $k = 1/N_\tau$.

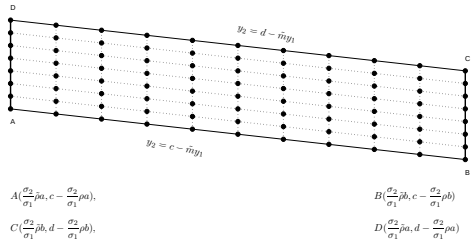

Figure 1: Rhomboid numerical domain $ABCD$.

As we mentioned in the introduction we are going to use Gauss-Hermite quadrature to discretize the integral part. So for the sake of convenience if we denote

by $\Phi = \{(\phi_{1,\ell}, \phi_{2,m}),\ 1 \le \ell \le L, 1 \le m \le M\}$ the set of all the pairs of zeroes of Hermite polynomial of degrees L in the first argument and M in the second respectively, we select parameters a, b, c, d identifying the rhomboid numerical domain Ω so that $\Phi \subset \Omega$ after L and M are prefixed.

Let us denote the approximation of $V(y_{1,i}, y^i_{2,j}, \tau^n)$ by $V^n_{i,j}$. Central finite difference approximations are used for the first and second spatial derivatives as follows

$$\begin{aligned} \frac{\partial V}{\partial y_1}(y_{1,i}, y^i_{2,j}, \tau^n) &\approx \frac{V^n_{i+1,j} - V^n_{i-1,j}}{2h_1}; \\ \frac{\partial V}{\partial y_2}(y_{1,i}, y^i_{2,j}, \tau^n) &\approx \frac{V^n_{i,j+1} - V^n_{i,j-1}}{2h_2}, \end{aligned} \tag{17}$$

$$\begin{aligned} \frac{\partial^2 V}{\partial y_1^2}(y_{1,i}, y^i_{2,j}, \tau^n) &\approx \frac{V^n_{i+1,j} - 2V^n_{i,j} + V^n_{i-1,j}}{h_1^2}; \\ \frac{\partial^2 V}{\partial y_2^2}(y_{1,i}, y^i_{2,j}, \tau^n) &\approx \frac{V^n_{i,j+1} - 2V^n_{i,j} + V^n_{i,j-1}}{h_2^2}, \end{aligned} \tag{18}$$

and forward finite difference approximation is implemented to approximate the time partial derivative of V

$$\frac{\partial V}{\partial \tau}(y_{1,i}, y^i_{2,j}, \tau^n) \approx \frac{V^{n+1}_{i,j} - V^n_{i,j}}{k}. \tag{19}$$

Once discretized the differential part of (12), we proceed to discretize the integral part. We recall the Gauss-Hermite quadrature in 2D for a function $z(x, y)$ given by

$$\mathbf{W}_L \mathbf{Z} \mathbf{W}_M^T = \sum_{l=1}^{L} \sum_{m=1}^{M} \omega_l \omega_m z_{lm} \approx \int_{-\infty}^{\infty} \int_{-\infty}^{\infty} e^{-(x^2+y^2)} z(x, y) dx dy, \tag{20}$$

$$\mathbf{W}_\alpha = [\omega_1 \ \ \omega_2 \ \ \ldots \ \ \omega_\alpha], \quad \alpha = L,\ M, \tag{21}$$

where ω_i, $i = 1, 2, \ldots, L$ for $\mathbf{W}_L$ and ω_i, $i = 1, 2, \ldots, M$ for $\mathbf{W}_M$ represent the corresponding weights for the roots of Hermite polynomial of degrees L and M respectively. $\mathbf{Z} = (z_{lm})$ is a matrix in $\mathbb{R}^{L \times M}$ and $z_{lm} = z(x_l, y_m)$ represents the value of the integrand function at node (x_l, y_m) for x_l, $1 \le l \le L$ and y_m,

$1 \leq m \leq M$ being the roots of Hermite polynomials of degrees L and M [18]. By applying formula (20) to the improper double integral of (12), one gets

$$\hat{I}_{i,j}^n = \sum_{\ell=1}^{L} \sum_{m=1}^{M} \omega_\ell \omega_m \mathcal{C}_{\ell m}(i,j) V^n(\phi_{1,\ell}, \phi_{2,m}), \tag{22}$$

where

$$\mathcal{C}_{\ell m}(i,j) = g(\frac{\sigma_1}{\sigma_2 \tilde{\rho}}(\phi_{1,\ell} - y_{1,i}), \phi_{2,m} - y_{2,j}^i + \tilde{m}(\phi_{1,\ell} - y_{1,i})) \exp[\phi_{1,\ell}^2 + \phi_{2,m}^2], \tag{23}$$

and $V^n(\phi_{1,\ell}, \phi_{2,m})$ denotes the approximate value of V at point $(\phi_{1,\ell}, \phi_{2,m}, \tau^n)$. Note that expression (22) involves evaluation at points that usually are different from those of the grid $(y_{1,i}, y_{2,j}^i),\ 1 \leq i \leq N_1,\ 1 \leq j \leq N_2$, and thus need to be interpolated. For each value $V^n(\phi_{1,\ell}, \phi_{2,m})$ appearing in (22) we want to locate the pair $(\phi_{1,\ell}, \phi_{2,m})$ in one of sub-rhomboids of the rhomboid grid. Let us denote such sub-rhomboid as $R(i_\ell, j_m^{i_\ell})$ in such way that the point $(\phi_{1,\ell}, \phi_{2,m})$ does not lie in the right-up sides of the sub-rhomboid. Rhomboid vertices of $R(i_\ell, j_m^{i_\ell})$ are given by $(y_{1,i_\ell}, y_{2,j_m}^{i_\ell})$, $(y_{1,i_\ell+1}, y_{2,j_m}^{i_\ell+1})$, $(y_{1,i_\ell+1}, y_{2,j_m+1}^{i_\ell+1})$ and $(y_{1,i_\ell}, y_{2,j_m+1}^{i_\ell})$. Following the idea of the bivariate interpolation four point formula [18, Ch. 25, p. 882], we modify such approximation for the rhomboid in Fig. 2 as follows,

$$\begin{aligned} V^n(\phi_{1,\ell}, \phi_{2,m}) \approx & \hat{\delta}_{i_\ell,2}(\delta_{j_m,2} V_{i_\ell,j_m}^n + \delta_{j_m,1} V_{i_\ell,j_m+1}^n) \\ & + \hat{\delta}_{i_\ell,1}(\delta_{j_m,3} V_{i_\ell+1,j_m+1}^n + \delta_{j_m,4} V_{i_\ell+1,j_m}^n), \end{aligned} \tag{24}$$

where

$$\begin{aligned} & \hat{\delta}_{i_\ell,1} = \tfrac{\phi_{1,\ell} - y_{1,i_\ell}}{h_1};\quad \hat{\delta}_{i_\ell,2} = \tfrac{y_{1,i_\ell+1} - \phi_{1,\ell}}{h_1};\quad \delta_{j_m,1} = \tfrac{\phi_{2,m} - y_{2,j_m}^{i_\ell}}{h_2}; \\ & \delta_{j_m,2} = \tfrac{y_{2,j_m+1}^{i_\ell} - \phi_{2,m}}{h_2};\quad \delta_{j_m,3} = \tfrac{\phi_{2,m} - y_{2,j_m}^{i_\ell+1}}{h_2};\ \delta_{j_m,4} = \tfrac{y_{2,j_m+1}^{i_\ell+1} - \phi_{2,m}}{h_2}. \end{aligned} \tag{25}$$

Consequently, the approximation of the integral part is obtained by substituting (24) into (22) ($I_{i,j}^n \approx \hat{I}_{i,j}^n$). Hence

$$\begin{aligned} I_{i,j}^n = & \sum_{\ell=1}^{L} \sum_{m=1}^{M} \beta_{i_\ell,j_m}^{(i,j)} V_{i_\ell,j_m}^n + \hat{\beta}_{i_\ell,j_m+1}^{(i,j)} V_{i_\ell,j_m+1}^n \\ & + \tilde{\beta}_{i_\ell+1,j_m}^{(i,j)} V_{i_\ell+1,j_m}^n + \breve{\beta}_{i_\ell+1,j_m+1}^{(i,j)} V_{i_\ell+1,j_m+1}^n, \end{aligned} \tag{26}$$

where

$$\begin{aligned}
\beta^{(i,j)}_{i_\ell,j_m} &= \omega_\ell\omega_m\mathcal{C}_{\ell m}(i,j)\hat{\delta}_{i_\ell,2}\delta_{j_m,2},\\
\hat{\beta}^{(i,j)}_{i_\ell,j_m+1} &= \omega_\ell\omega_m\mathcal{C}_{\ell m}(i,j)\hat{\delta}_{i_\ell,2}\delta_{j_m,1},\\
\tilde{\beta}^{(i,j)}_{i_\ell+1,j_m} &= \omega_\ell\omega_m\mathcal{C}_{\ell m}(i,j)\hat{\delta}_{i_\ell,1}\delta_{j_m,4},\\
\breve{\beta}^{(i,j)}_{i_\ell+1,j_m+1} &= \omega_\ell\omega_m\mathcal{C}_{\ell m}(i,j)\hat{\delta}_{i_\ell,1}\delta_{j_m,3}.
\end{aligned} \tag{27}$$

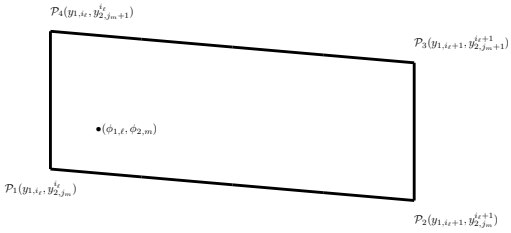

Figure 2: Neighbor coordinate points to $(\phi_{1,\ell}, \phi_{2,m})$.

Note that given Φ we can always choose values of h_1 and h_2 such that coefficients in (25) are nonnegative and thus the resulting 2D interpolation formula is also nonnegative. From (18)-(26), the corresponding finite difference scheme becomes

$$V^{n+1}_{i,j} = \alpha_1 V^n_{i-1,j} + \alpha_2 V^n_{i,j-1} + \alpha_3 V^n_{i,j} + \alpha_4 V^n_{i,j+1} + \alpha_5 V^n_{i+1,j} + \frac{k\lambda\sigma_1}{\sigma_2\tilde{\rho}} I^n_{i,j}, \tag{28}$$

$$\begin{aligned}
V^n_{i,0} = e^{\lambda\tau^n},\ V^n_{0,j} = e^{\lambda\tau^n},\ V^n_{N_1,j} = f_{N_1,j},\\
V^n_{i,N_2} = f_{i,N_2},\ 1 \le i \le N_1,\ 1 \le j \le N_2,
\end{aligned} \tag{29}$$

where

$$\begin{aligned}
&\alpha_1 = \tfrac{k}{2h_1}(\tfrac{\sigma_2^2\tilde{\rho}^2}{h_1} - a_1);\quad \alpha_2 = \tfrac{k}{2h_2}(\tfrac{\sigma_2^2\tilde{\rho}^2}{h_2} - a_2);\\
&\alpha_3 = 1 - k\sigma_2^2\tilde{\rho}^2(\tfrac{1}{h_1^2} + \tfrac{1}{h_2^2});\quad \alpha_4 = \tfrac{k}{2h_2}(\tfrac{\sigma_2^2\tilde{\rho}^2}{h_2} + a_2);\\
&\alpha_5 = \tfrac{k}{2h_1}(\tfrac{\sigma_2^2\tilde{\rho}^2}{h_1} + a_1).
\end{aligned} \tag{30}$$

4. Positivity and stability

Dealing with prices, reliable numerical solution needs to be nonnegative. In this section we study the positivity of the numerical solution of the problem computed throughout the scheme (28). As we show at the end of the previous Section, the quadrature and interpolation procedure achieving the approximation $I_{i,j}^n$ appearing in (28) provide nonnegative values. Thus in order to guarantee positivity of the numerical solution computed throughout the scheme (28), it is sufficient to show that coefficients α_i, $i = 1, \dots 5$, are nonnegative together with nonnegativity of the initial and boundary conditions (14). From (30), it is easy to check that under the conditions

$$k < \frac{h_1^2 h_2^2}{\sigma_2^2 \tilde{\rho}^2 (h_1^2 + h_2^2)}, \quad h_1 < \frac{\sigma_2^2 \tilde{\rho}^2}{|a_1|}, \quad h_2 < \frac{\sigma_2^2 \tilde{\rho}^2}{|a_2|}, \tag{31}$$

the coefficients of $\alpha_i,\ 1 \leq i \leq 5$ are nonnegative. For the sake of clarity in the presentation we recall the definition of stability used in this paper previously used in [15].

Definition 1. Consider a numerical solution $\{V_{i,j}^n\}$ of the PIDE computed from the scheme (28)-(30) with stepsizes $h_1 = \Delta y_1$, $h_2 = \Delta y_2$ in a rhomboid computational domain and $k = \Delta\tau$. From one hand it is said that $\{V_{i,j}^n\}$ is strongly uniformly $\|.\|_\infty$ stable, if the vector solution $\mathbf{V}^n$ satisfies

$$\|\mathbf{V}^n\|_\infty \leq \Upsilon \|\mathbf{V}^0\|_\infty, \quad 0 \leq n \leq N_\tau, \tag{32}$$

where $\Upsilon > 0$ does not depend on the stepsizes h_1, h_2 and k.
On the other hand it is said to be conditionally stable when Υ is obtained under a certain condition on the stepsizes.

Following the technique of block matrices [21, 15], the finite difference scheme (28)-(30) is written in the following form.

$$\mathbf{V}^n = [\mathcal{V}_0^n\ \mathcal{V}_1^n \dots \mathcal{V}_{N_1}^n]^T,\ \mathcal{V}_i^n = [V_{i,0}^n\ V_{i,1}^n \dots V_{i,N_2}^n]. \tag{33}$$

The matrix representation of scheme (28)-(30) is given by

$$\mathbf{V}^{n+1} = (\mathcal{A} + \mathcal{B})\mathbf{V}^n, \tag{34}$$

where $\mathcal{A}$ and $\mathcal{B}$ are square matrices of size $(N_1+1)(N_2+1)\times(N_1+1)(N_2+1)$ representing the discretization of the differential and integral operators. The matrix $\mathcal{A}$ is given by

$$\mathcal{A}=\begin{bmatrix} e^{k\lambda}I & \Theta & \Theta & \Theta & \dots & \dots & \Theta \\ \breve{A} & A & \hat{A} & \Theta & \dots & \dots & \Theta \\ \Theta & \breve{A} & A & \hat{A} & \Theta & \dots & \Theta \\ \vdots & \Theta & \ddots & \ddots & \ddots & \vdots & \vdots \\ \vdots & \vdots & \ddots & \ddots & \ddots & \ddots & \vdots \\ \vdots & \vdots & \dots & \Theta & \breve{A} & A & \hat{A} \\ \Theta & \Theta & \dots & \dots & \dots & \dots & I \end{bmatrix}, \tag{35}$$

where I and Θ are the identity and zero matrices of size $(N_2+1)\times(N_2+1)$. The block entries $\breve{A}=(\breve{a}_{ij})$, $A=(a_{ij})$ and $\hat{A}=(\hat{a}_{ij})$ are $(N_2+1)\times(N_2+1)$ matrices such that

$$\begin{aligned} \breve{a}_{ij} &= \begin{cases} \alpha_1, & i=j=2,3,\dots N_2-1, \\ 1, & i=j=N_2+1, \\ 0, & \text{otherwise.} \end{cases}, \\ \hat{a}_{ij} &= \begin{cases} \alpha_5, & i=j=2,3,\dots N_2-1, \\ 1, & i=j=N_2+1, \\ 0, & \text{otherwise.} \end{cases}, \\ a_{ij} &= \begin{cases} e^{k\lambda}, & i=j=1, \\ \alpha_2, & j=i-1,\ i=2,3,\dots N_2-1, \\ \alpha_3, & j=i,\ i=2,3,\dots N_2-1, \\ \alpha_4, & j=i+1,\ i=2,3,\dots N_2-1, \\ 1, & i=j=N_2+1 \\ 0, & \text{otherwise.} \end{cases} \end{aligned} \tag{36}$$

The square matrix $\mathcal{B}$ is a sparse block matrix containing $(N_1+1)\times(N_1+1)$ block entries of size $(N_2+1)\times(N_2+1)$. From the Gauss-Hermite quadrature together with the bivariate interpolation technique used, the nonzero blocks of $\mathcal{B}$ are located at block positions with row indices i_1, i_1+1, i_2, i_2+1, …, i_L, i_L+1

and column indices j_1, j_1+1, j_2, j_2+1, $\ldots$, j_M, j_M+1. Let $B(i_\ell) = (b_{l_1 l_2}(i_\ell))$ and $B(i_\ell+1) = (b_{l_1 l_2}(i_\ell+1))$ denote the non zero blocks in the matrix $\mathcal{B}$ with entries given by

$$b_{l_1 l_2}(i_\ell) = \begin{cases} \hat{\lambda}\beta^{(i,j)}_{i_\ell,l_2}, & l_1 = 2,3,\ldots,N_2,\ l_2 = j_1, j_2, \ldots, j_M, \\ \hat{\lambda}\hat{\beta}^{(i,j)}_{i_\ell,l_2}, & l_1 = 2,3,\ldots,N_2,\ l_2 = j_1+1, j_2+1, \ldots, j_M+1, \\ 0, & \text{otherwise}, \end{cases}$$

$$b_{l_1 l_2}(i_\ell+1) = \begin{cases} \hat{\lambda}\tilde{\beta}^{(i,j)}_{i_\ell+1,l_2}, & l_1 = 2,\ldots,N_2,\ l_2 = j_1, j_2, \ldots, j_M, \\ \hat{\lambda}\breve{\beta}^{(i,j)}_{i_\ell+1,l_2}, & l_1 = 2,\ldots,N_2,\ l_2 = j_1+1, \ldots, j_M+1, \\ 0, & \text{otherwise}, \end{cases} \tag{37}$$

where $\hat{\lambda} = \frac{k\lambda\sigma_1}{\sigma_2\tilde{\rho}}$. Note that the indices (i,j) change depending on the corresponding indices in $V^{n+1}_{i,j}$. By calculating the infinite norm for matrix $\mathcal{A}$ under the positivity conditions (31), we have

$$\|\mathcal{A}\|_\infty = \max\{e^{k\lambda}, \sum_{i=1}^{5}|\alpha_i|\} = \max\{e^{k\lambda}, 1\} = e^{k\lambda}. \tag{38}$$

Infinite norm of the matrix $\mathcal{B}$ verifies

$$\|\mathcal{B}\|_\infty = \sum_{l_2=1}^{\hat{N}} |b_{i_f l_2}| = \hat{\lambda}\sum_{\ell=1}^{L}\sum_{m=1}^{M}(\beta^{(i_f,j)}_{i_\ell,j_m} + \hat{\beta}^{(i_f,j)}_{i_\ell,j_m+1} + \tilde{\beta}^{(i_f,j)}_{i_\ell+1,j_m} + \breve{\beta}^{(i_f,j)}_{i_\ell+1,j_m+1}), \tag{39}$$

where i_f denotes the rank of row that contains the highest sum, $\hat{N} = (N_1+1)(N_2+1)$. From equations (27) and (25), the coefficients $\hat{\delta}_{i_\ell,1}$, $\hat{\delta}_{i_\ell,2}$, $\delta_{j_m,1}$, $\delta_{j_m,2}$, $\delta_{j_m,3}$ and $\delta_{j_m,4}$ do not exceed 1. Consequently,

$$\|\mathcal{B}\|_\infty \leq \frac{4k\lambda\sigma_1}{\sigma_2\tilde{\rho}}\sum_{\ell=1}^{L}\sum_{m=1}^{M}\omega_\ell\omega_m\mathcal{C}_{\ell m}(i_f, j). \tag{40}$$

The double summation in (40) is an approximation to the double integration of $g(\frac{\sigma_1}{\sigma_2\tilde{\rho}}(\phi_1 - y_{1,i_f}), \phi_2 - y^{i_f}_{2,j} + \tilde{m}(\phi_1 - y_{1,i_f}))$ with respect to ϕ_1 and ϕ_2, hence for arbitrary small $\epsilon > 0$ there exist large enough values L and M such that

$$\begin{aligned} &\sum_{\ell=1}^{L}\sum_{m=1}^{M}\omega_\ell\omega_m\mathcal{C}_{\ell m}(i,j) \\ &\qquad < \epsilon + \int_{\mathbb{R}^2} g(\frac{\sigma_1}{\sigma_2\tilde{\rho}}(\phi_1 - y_{1,i}), \phi_2 - y^{i}_{2,j} + \tilde{m}(\phi_1 - y_{1,i}))d\phi_1 d\phi_2. \end{aligned} \tag{41}$$

Taking into account that the value of the improper integral in (41) is $\frac{\sigma_2\tilde{\rho}}{\sigma_1}$, norm of matrix $\mathcal{B}$ is bounded since

$$\|\mathcal{B}\|_\infty \leq 4k\lambda\left(1+\frac{\sigma_1\epsilon}{\sigma_2\tilde{\rho}}\right) = 4k\lambda^*. \tag{42}$$

By taking the infinite norm in equation (34), we have

$$\|\mathbf{V}^{n+1}\|_\infty \leq (\|\mathcal{A}\|_\infty + \|\mathcal{B}\|_\infty)\|\mathbf{V}^n\|_\infty,\ n=0,1,\ldots,N_\tau-1, \tag{43}$$

$$\begin{aligned}\|\mathbf{V}^{N_\tau}\|_\infty &\leq (e^{k\lambda}+4k\lambda^*)^{N_\tau}\|\mathbf{V}^0\|_\infty = e^{\lambda}(1+4k\lambda^* e^{-k\lambda})^{N_\tau}\|\mathbf{V}^0\|_\infty.\\ &\leq e^{\lambda}(1+4k\lambda^*)^{N_\tau}\|\mathbf{V}^0\|_\infty \leq e^{\lambda+4\lambda^*}\|\mathbf{V}^0\|_\infty,\end{aligned} \tag{44}$$

and from definition 1, a conditional strong uniform stable scheme is established.

5. Consistency

The proposed scheme (28) is said to be consistent with PIDE (12), if the exact theoretical solution approximates well the difference scheme as the discretization stepsizes tend to zero [22]. Let us denote $v^n_{i,j} = V(y_{1,i}, y^j_{2,i}, \tau^n)$ the exact solution of the PIDE at point $(y_{1,i}, y^i_{2,j}, \tau^n)$. The associated local truncation error $T^n_{i,j}(V)$ is given by

$$T^n_{i,j}(V) = L(V^n_{i,j}) - \mathcal{I}(V^n_{i,j}), \tag{45}$$

where $L(V^n_{i,j})$ and $\mathcal{I}(V^n_{i,j})$ are the truncation errors for the differential and integral parts respectively denoted by

$$\begin{aligned}L(V^n_{i,j}) = &\frac{v^{n+1}_{i,j}-v^n_{i,j}}{k}\\ &-\frac{\sigma_2^2\tilde{\rho}^2}{2}\left(\frac{v^n_{i+1,j}-2v^n_{i,j}+v^n_{i-1,j}}{h_1^2}+\frac{v^n_{i,j+1}-2v^n_{i,j}+v^n_{i,j-1}}{h_2^2}\right)\\ &-\left(a_1\left(\frac{v^n_{i+1,j}-v^n_{i-1,j}}{2h_1}\right)+a_2\left(\frac{v^n_{i,j+1}-v^n_{i,j-1}}{2h_2}\right)\right)\\ &-\left(\frac{\partial V}{\partial\tau}-\frac{\sigma_2^2\tilde{\rho}^2}{2}\left(\frac{\partial^2 V}{\partial y_1^2}-\frac{\partial^2 V}{\partial y_2^2}\right)-a_1\frac{\partial V}{\partial y_1}-a_2\frac{\partial V}{\partial y_2}\right)\Bigg|_{(y_{1,i},y^i_{2,j},\tau^n)},\end{aligned} \tag{46}$$

$$\mathcal{I}(V_{i,j}^n) = \frac{\sigma_1\lambda}{\sigma_2\tilde{\rho}}\left(I(v_{i,j}^n) - F(y_{1,i}, y_{2,j}^i, \tau^n)\right), \tag{47}$$

where

$$\begin{aligned} &F(y_{1,i}, y_{2,j}^i, \tau^n) = \\ &\int_{\mathbb{R}^2} V(\phi_1, \phi_2, \tau^n) g(\frac{\sigma_1}{\sigma_2\tilde{\rho}}(\phi_1 - y_{1,i}), \phi_2 - y_{2,j}^i + \tilde{m}(\phi_1 - y_{1,i}))d\phi_1 d\phi_2, \end{aligned} \tag{48}$$

$I(v_{i,j}^n)$ denotes the corresponding value by replacing in the expression of $I_{i,j}^n$ appearing in (28), the value of the numerical solution at the vertices of each $R(i_\ell, j_m)$ by the exact solution value v at the corresponding nodes. Thus consistency of scheme (28) with the PIDE (12) means that local truncation error $T_{i,j}^n$ tends to zero as the stepsize discretization h_1, h_2 and k tend to zero and the degree of Hermite polynomials tend to infinity.

Assuming that the exact solution is twice continuously differentiable with respect to τ and four times for the spatial variables y_1 and y_2 and using Taylor expansion about $(y_{1,i}, y_{2,j}^i, \tau^n)$, it is not difficult, see [15], to show that

$$L(V_{i,j}^n) = \mathcal{O}(h_1^2) + \mathcal{O}(h_2^2) + \mathcal{O}(k). \tag{49}$$

With respect to the discretization error of the integral part, one gets

$$\mathcal{I}(V_{i,j}^n) = \frac{\sigma_1\lambda}{\sigma_2\tilde{\rho}}\left[\left(I(v_{i,j}^n) - \hat{I}_{i,j}^n(v)\right) + \left(\hat{I}_{i,j}^n(v) - F(y_{1,i}, y_{2,j}^i, \tau^n)\right)\right], \tag{50}$$

where $\hat{I}_{i,j}^n(v)$ represents the value of (22) by replacing the value $V^n(\phi_{1,\ell}, \phi_{2,m})$ by the exact solution value $V(\phi_{1,\ell}, \phi_{2,m}, \tau^n)$. The first bracket of (50) denotes the difference between the quadrature formula evaluated at root points $(\phi_{1,\ell}, \phi_{2,m})$ of Hermite polynomial and the formula using linear bivariate interpolation with respect to the vertices of the rhomboid $R(i_\ell, j_m^{i_\ell})$ that contains this point $(\phi_{1,\ell}, \phi_{2,m})$. From [18],

$$I(v_{i,j}^n) - \hat{I}_{i,j}^n(v) = \mathcal{O}(h_1^2) + \mathcal{O}(h_2^2). \tag{51}$$

The second bracket in the right hand side of (50) represents the associated quadrature error of the 2D Hermite-Gauss quadrature formula and from [23],

one gets

$$\hat{I}^n_{i,j}(v) - F(y_{1,i}, y^i_{2,j}, \tau^n) = \epsilon_1(L) + \epsilon_2(M) + \mathcal{O}(\epsilon_1\epsilon_2), \tag{52}$$

with

$$\begin{aligned} &\epsilon_1(L) = L!^2 \max_{\phi_2} \hat{f}([\phi_{1,1}, \phi_{1,1}, \phi_{1,2}, \phi_{1,2}, \ldots, \phi_{1,L}, \phi_{1,L}, \xi_1], \phi_2), \\ &\epsilon_2(M) = M!^2 \max_{\phi_1} \hat{f}(\phi_1, [\phi_{2,1}, \phi_{2,1}, \phi_{2,2}, \phi_{2,2}, \ldots, \phi_{2,M}, \phi_{2,M}, \xi_2]), \end{aligned} \tag{53}$$

where $\hat{f}$ denotes the integrand function in (48) and $f[x_1, x_1, x_2, \ldots, x_m, x_m, \xi]$ is the divided difference with respect to variable x. For smooth enough integrand functions the error takes the form [23]

$$|\hat{I}^n_{i,j}(v) - F(y_{1,i}, y^i_{2,j}, \tau^n)| = \frac{(L!)^2}{2L!} \left| \frac{\partial^{2L} \hat{f}}{\partial \phi_1^{2L}} \right|_{(\xi_1, \phi_2)} + \frac{(M!)^2}{2M!} \left| \frac{\partial^{2M} \hat{f}}{\partial \phi_2^{2M}} \right|_{(\phi_1, \hat{\xi_2})} + \mathcal{O}(\epsilon_1\epsilon_2).$$

6. The American option case

Since the option of American type can be exercised during any time until the maturity date, the model is constituted by a linear complementary problem (LCP) [24, 25] given by

$$\mathcal{L}[V] \geq 0,\ V \geq f(x_1, x_2),\ \mathcal{L}[V](V - f(x_1, x_2)) = 0, \tag{54}$$

where

$$\begin{aligned} &\mathcal{L}[V] = \tfrac{\partial V}{\partial \tau} - \mathcal{D}[V] - I[V], \\ &\mathcal{D}[V] = \tfrac{\sigma_2^2 \tilde{\rho}^2}{2} \left(\tfrac{\partial^2 V}{\partial y_1^2} + \tfrac{\partial^2 V}{\partial y_2^2} \right) + a_1 \tfrac{\partial V}{\partial y_1} + a_2 \tfrac{\partial V}{\partial y_2}, \\ &I[V] = \\ &\tfrac{\sigma_1 \lambda}{\sigma_2 \tilde{\rho}} \int_{\mathbb{R}^2} V(\phi_1, \phi_2, \tau) g(\tfrac{\sigma_1}{\sigma_2 \tilde{\rho}}(\phi_1 - y_1), \phi_2 - y_2 + \tilde{m}(\phi_1 - y_1)) d\phi_1 d\phi_2. \end{aligned} \tag{55}$$

Solving LCP (54) numerically using explicit scheme requires a large amount of computations. Here we propose an alternative way to discretize the derivative of V with respect to time. Firstly we use the semi-discrete formulation of problem (55) as follows

$$\mathcal{D}[V] \approx \tilde{\alpha}_1 V_{i+1,j} - \tilde{\alpha}_2 V_{i,j} + \tilde{\alpha}_3 V_{i-1,j} + \tilde{\alpha}_4 V_{i,j+1} + \tilde{\alpha}_5 V_{i,j-1}, \tag{56}$$

where

$$\begin{aligned}\tilde{\alpha}_1 &= \left(\frac{\sigma_2^2\tilde{\rho}^2}{2h_1^2} + \frac{a_1}{2h_1}\right),\ \tilde{\alpha}_2 = \sigma_2^2\tilde{\rho}^2\left(\frac{1}{h_1^2} + \frac{1}{h_2^2}\right),\ \tilde{\alpha}_3 = \left(\frac{\sigma_2^2\tilde{\rho}^2}{2h_1^2} - \frac{a_1}{2h_1}\right)\\ \tilde{\alpha}_4 &= \left(\frac{\sigma_2^2\tilde{\rho}^2}{2h_2^2} + \frac{a_2}{2h_2}\right),\ \tilde{\alpha}_5 = \left(\frac{\sigma_2^2\tilde{\rho}^2}{2h_2^2} - \frac{a_2}{2h_2}\right).\end{aligned} \tag{57}$$

The integral operator $I[V]$ is discretizated in space analogously as in (26). Let $\mathcal{F}$ be a $(N_1-1)(N_2-1)\times(N_1-1)(N_2-1)$ matrix containing the coefficients of the differential and integral operators approximations. Hence the semi-discrete approximation of (54) takes the form

$$\frac{\partial \mathbf{V}}{\partial \tau} + \mathcal{F}\mathbf{V} \geq \mathbf{b};\ \mathbf{V} \geq \mathbf{f};\ \left(\frac{\partial \mathbf{V}}{\partial \tau} + \mathcal{F}\mathbf{V} - \mathbf{b}\right)^T(\mathbf{V}-\mathbf{f}) = 0, \tag{58}$$

where

$$\begin{aligned}&\mathbf{V} = [\mathcal{V}_1,\ \mathcal{V}_2, \ldots, \mathcal{V}_{N_1-1}]^T,\ \mathcal{V}_i = [V_{i,1},\ V_{i,2}, \ldots, V_{i,N_2-1}],\\ &\mathbf{f} = [\breve{\mathbf{f}}_1,\ \breve{\mathbf{f}}_2, \ldots, \breve{\mathbf{f}}_{N_1-1}]^T,\ \breve{\mathbf{f}}_i = [f_{i,1},\ f_{i,2}, \ldots, f_{i,N_2-1}],\\ &\qquad i = 1, 2, \ldots, N_1-1,\\ &\mathbf{b} = [\mathcal{V}_0, \mathbf{0}, \ldots, \mathbf{0}, \mathcal{V}_{N_1}]^T,\ \mathcal{V}_i = [V_{i,1}, V_{i,2}, \ldots, V_{i,N_2-1}],\\ &\qquad i = 1, N_1,\ \mathbf{0} \in \mathbb{R}^{N_2-1}.\end{aligned} \tag{59}$$

Three or more time-level schemes can be used to achieve some advantage versus two-level schemes, such as better stability behavior, more accurate local consistency or transforming a nonlinear problem into a linear one [22]. Here the three time-level scheme is used to solve the full discretization of (54), that leads to the sequence of LCPs denoted by

$$LCP(\hat{\mathcal{F}},\ \mathbf{V}^{n+1},\ \tilde{\mathbf{V}}^n, \mathbf{f}), \tag{60}$$

and given by

$$\hat{\mathcal{F}}\mathbf{V}^{n+1} - \tilde{\mathbf{V}}^n \geq 0, \quad \mathbf{V}^{n+1} \geq \mathbf{f}, \quad \left(\hat{\mathcal{F}}\mathbf{V}^{n+1} - \tilde{\mathbf{V}}^n\right)\left(\mathbf{V}^{n+1} - \mathbf{f}\right) = 0, \tag{61}$$

where

$$\hat{\mathcal{F}} = \begin{cases} I + k\mathcal{F} & n = 0,\\ I + \frac{2k}{3}\mathcal{F} & n \geq 1,\end{cases} \tag{62}$$

$$\tilde{\mathbf{V}}^n = \begin{cases} \mathbf{V}^0 + k\mathbf{b}, & n = 0,\\ \frac{4}{3}\mathbf{V}^n - \frac{1}{3}\mathbf{V}^{n-1} + \frac{2k}{3}\mathbf{b} & n \geq 1.\end{cases} \tag{63}$$

Note that in order to solve (60) using three time-level, the first two level solutions $\mathbf{V}^0$ and $\mathbf{V}^1$ must be known. The vector $\mathbf{V}^0$ corresponds to the initial condition which is given while $\mathbf{V}^1$ is an unknown vector. So before implementing the three time-level, this vector must be obtained using another method, here the implicit Euler approximation has been used as shown in the first branch in (62) and (63). Note that $\hat{\mathcal{F}}$ is an M-Matrix.

The arising LCP is solved using two different methods; the projected successive over relaxation (**PSOR**) and multigrid (**MG**) techniques. In **PSOR** introduced by Cryer [26], the solution vector components are relaxed several times with a projection to any component has a value less than the payoff. This relaxation process can be accelerated using a parameter $\omega \in (0, 2)$. Using **MG** techniques, the initial guess is improved using coarser and finer grids. The problem is mapped to the coarse grid, after that the iteration is done to obtain the vector solution [27, 28, 29, 30].

7. Numerical Examples

Results of the proposed schemes are illustrated with four examples comparing and discussing the results for European and American put options on the minimum of two asset. The numerical examples are executed using Matlab on a Microprocessor 2.8 GHz Intel Core i5.

Example 1. Here we compare the value of European put options obtained using scheme (28)-(30) with the reference values in [5]. Consider an European put option with parameters $T = 1$, $E = 100$, $r = 0.05$, $q_1 = q_2 = 0$, $\sigma_1 = 0.12$, $\sigma_2 = 0.15$, $\rho = 0.3$, $\lambda = 0.6$, $\mu_1 = -0.1$, $\mu_2 = 0.1$, $\hat{\sigma}_1 = 0.17$, $\hat{\sigma}_2 = 0.13$, $\rho_J = -0.2$ and the boundaries x_1x_2-plane are $x_1, x_2 \in [-3, 3]$. The root mean square relative error (**RMSRE**) for S_1, S_2 belonging to the set $\{90, 100, 110\}$ is calculated for $L = M = 3$ and 5. The reference values are taken from [5] and the **RMSRE** is obtained for three groups $\hat{S}_1 = \{(90, 90), (90, 100), (90, 110)\}$, $\hat{S}_2 = \{(100, 90), (100, 100), (100, 110)\}$ and $\hat{S}_3 = \{(110, 90), (110, 100), (110, 110)\}$. Table 1 reports the associated **RMSRE**, ra-

		$\hat{S}_1$		$\hat{S}_2$		$\hat{S}_3$		CPU
	(N_1, N_2, N_τ)	**RMSRE**	Ratio	**RMSRE**	Ratio	**RMSRE**	Ratio	(sec)
$L = M = 3$	(64,32,50)	4.188e-3	–	3.561e-3	–	4.755e-3	–	0.17
	(128,64,100)	1.247e-3	3.11	1.197e-3	2.97	2.016e-3	2.36	2.63
	(256,128,200)	8.836e-4	1.41	7.158e-4	1.67	7.241e-4	2.78	10.72
	(512,256, 400)	2.480e-4	3.48	1.742e-4	4.11	6.901e-5	3.64	59.17
$L = M = 5$	(64,32,50)	2.611e-3	–	3.558e-3	–	2.752e-3	–	0.31
	(128,64,100)	7.854e-4	3.32	8.205e-4	4.34	7.326e-4	3.76	2.72
	(256,128,200)	5.392e-4	1.45	4.916e-4	1.67	4.388e-4	1.67	11.12
	(512,256, 400)	1.369e-4	3.94	1.267e-4	3.88	1.040e-4	4.22	64.39

Table 1: The **RMSRE** for European put option on the minimum of two assets for several grids.

tio and CPU time for several grids.

The next example shows the importance of positivity conditions (31) getting wrong results when they are broken.

Example 2. Here the parameters for European put option are $T = 1$, $E = 100$, $r = 0.1$, $q_1 = q_2 = 0$, $\sigma_1 = 0.15$, $\sigma_2 = 0.2$, $\rho = 0.4$, $\lambda = 0.2$, $\mu_1 = -0.2$, $\mu_2 = 0.15$, $\hat{\sigma}_1 = 0.2$, $\hat{\sigma}_2 = 0.3$ and $\rho_J = 0.4$. The option surface is plotted as a function of S_1 and S_2 for $(N_1, N_2, N_\tau) = (480, 240, 400)$ and $(480, 240, 100)$. The first ordered triplet represents the grid when the positivity conditions hold as shown in Fig. 3 while the second one does not satisfy them, see Fig. 4.

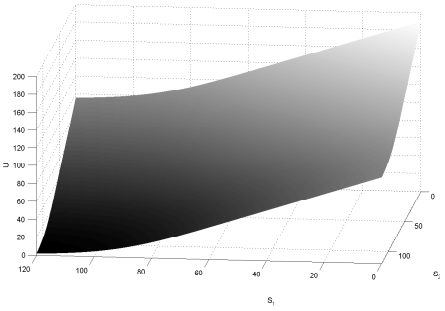

Figure 3: European put option: the positivity conditions hold.

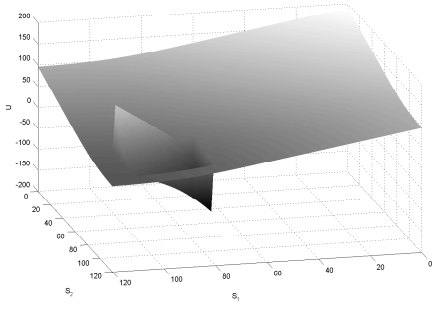

Figure 4: European put option: the positivity conditions are broken.

Next example shows the associated truncated error of the integral part (52) for several values of L and M.

		Errors for grids		
(L, M)	$(\hat{\xi}_1, \hat{\xi}_2)$	(60,30,50)	(240,120,200)	(480,240,400)
(3,5)	(-0.74,-1.85)	7.483e-3	2.186e-4	1.366e-6
	(0.58,-1.23)	-5.278e-3	7.214e-5	-8.349e-7
	(1.12,1.67)	8.769e-4	4.156e-5	1.227e-7
(10,10)	(-2.82,2.82)	-2.395e-6	6.238e-7	2.588e-10
	(-1.56,-1.56)	8.723e-8	-5.742e-9	-7.386e-11
	(2.63,3.15)	3.544e-8	-1.299e-9	4.715e-11
(15,20)	(-3.94,-5.18)	-3.148e-11	4.391e-13	-5.782e-15
	(-2.48,-4.37)	7.287e-12	-5.136e-14	6.394e-16
	(3.26,1.79)	2.157e-12	1.319e-14	-2.915e-16

Table 2: The truncated error for the integral part

Example 3. Based on equation (52) and (53) the associated error with the integral part approximation for given values of L and M can be controlled by using suitable values of $\hat{\xi}_1$ and $\hat{\xi}_2$ (53). Here the parameters are $T = 1$, $E = 100$, $r = 0.1$, $q_1 = q_2 = 0$, $\sigma_1 = 0.25$, $\sigma_2 = 0.15$, $\rho = -0.5$, $\lambda = 0.25$, $\mu_1 = -0.1$, $\mu_2 = 0.1$, $\hat{\sigma}_1 = 0.17$, $\hat{\sigma}_2 = 0.13$, $\rho_J = -0.2$ and the boundaries x_1x_2-plane are $x_1, x_2 \in [-6, 6]$. Table 2 reports the truncated error of the integral part for several grids, L and M. Moreover, the error can be minimized using suitable values of $\hat{\xi}_1$ and $\hat{\xi}_2$. In Table 2, we show accurate approximations for small numbers L and M of Hermite polynomials zeroes.

In next example 4 one performs a comparison between **PSOR** and **MG** methods for American options under jump diffusion on two assets.

Example 4. The prices for American put options are computed using scheme (60)-(63) and compared with the reference values in [5]. Here the parameters are the same as in Example 1, with $x_1, x_2 \in [-6, 6]$. Tables 3 and 4 report the errors solving scheme (60)-(63) by using **PSOR** and **MG** respectively. Also ratio and CPU time are shown.

Note that the ratios in Tables 3 and 4 are about 4. This fact is according with the second-order accuracy in both space and time due to the central approximations in space and the three time level discretization. The use of the first implicit Euler time step does not affect significantly the overall convergence.

In Fig. 5 the efficiency graph of the PSOR and MG methods is presented

		$\hat{S}_1$		$\hat{S}_2$		$\hat{S}_3$		CPU
	(N_1, N_2, N_τ)	**RMSRE**	Ratio	**RMSRE**	Ratio	**RMSRE**	Ratio	(sec)
$L = M = 6$	(64,32,32)	1.087e-2	–	1.460e-2	–	1.153e-2	–	0.36
	(128,64,64)	3.056e-3	3.56	4.247e-3	3.44	3.521e-3	3.27	5.62
	(256,128,128)	7.255e-4	4.21	1.123e-3	3.78	7.767e-4	4.53	40.48
	(512,256,256)	1.349e-4	5.38	2.147e-4	5.23	1.510e-4	5.14	220.17
$L = M = 10$	(64,32,32)	6.139e-3	–	9.476e-3	–	7.618e-3	–	0.44
	(128,64,64)	1.695e-3	3.62	2.885e-3	3.28	2.092e-3	3.64	6.25
	(256,128,128)	3.537e-4	4.79	6.110e-4	4.72	5.037e-4	4.15	52.37
	(512,256,256)	6.646e-5	5.32	1.104e-4	5.53	9.829e-5	5.12	247.68

Table 3: The **RMSRE** for American put option on the minimum of two assets for several grids using **PSOR**.

		$\hat{S}_1$		$\hat{S}_2$		$\hat{S}_3$		
	(N_1, N_2, N_τ)	**RMSRE**	Ratio	**RMSRE**	Ratio	**RMSRE**	Ratio	CPU (sec)
$L = M = 6$	(64,32,32)	3.837e-3	–	2.108e-3	–	1.866e-3	–	0.28
	(128,64,64)	9.183e-4	4.18	5.916e-4	3.56	5.343e-4	3.49	2.11
	(256,128,128)	1.982e-4	4.63	1.213e-4	4.88	1.117e-4	4.78	13.66
	(512,256,256)	3.590e-5	5.52	2.217e-5	5.47	1.923e-5	5.81	72.39
$L = M = 10$	(64,32,32)	1.055e-3	–	1.714e-3	–	1.338e-3	–	0.35
	(128,64,64)	2.456e-4	4.29	4.503e-4	3.81	3.412e-4	3.92	2.64
	(256,128,128)	5.401e-5	4.55	9.523e-5	4.73	7.467e-5	4.57	16.28
	(512,256,256)	9.372e-6	5.76	1.756e-5	5.42	1.252e-5	5.96	77.85

Table 4: The **RMSRE** for American put option on the minimum of two assets for several grids using **MG**.

taking into account the CPU time and the RMSRE for the set $\hat{S}_2$ in Tables 3 and 4. Because of a large range of quantities the logarithmic scale is used. MG tecnique shows more efficiency in terms of RMSE/CPU.

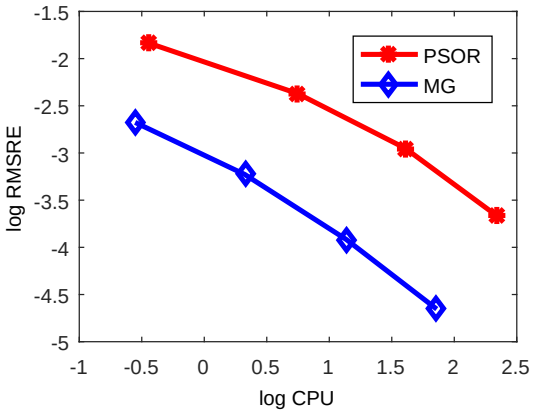

Figure 5: Efficiency graph of the PSOR and MG methods for $L = M = 6$.

Acknowledgements

This work has been partially supported by the European Union in the FP7-PEOPLE-2012-ITN program under Grant Agreement Number 304617 (FP7 Marie Curie Action, Project Multi-ITN STRIKE-Novel Methods in Computational Finance) and the Ministerio de Economía y Competitividad Spanish grant MTM2013-41765-P.

References

[1] B. Dupire, Arbitrage pricing with stochastic volatility, Tech. Rep., Banque Paribas Swaps and Options Research Team Monograph, 1993.

[2] R. Cont, P. Tankov, *Financial Modelling with Jump Processes*, CRC Financial Mathematics Series, Chapman and Hall, 2004.

[3] R. C. Merton, Option pricing when underlying stock returns are discontinuous, *Journal of Financial Economics* 3(1976) 125-144.

[4] S. G. Kou, A jump-diffusion model for option pricing, *Management Science*, 48(8) (2002) 1086-1101.

[5] S. S. Clift, P. A. Forsyth, Numerical solution of two asset jump diffusion models for option valuation, *Applied Numerical Mathematics* 58 (2008) 743–782.

[6] S. H. Martzoukos, Contingent claims on foreign assets following jump-diffusion processes, *Review of Derivatives Research* 6 (1) (2003) 27-45.

[7] K. I. Amin, Jump diffusion option valuation in discrete time, *Journal of Finance* 48 (5) (1993) 1833-1863.

[8] N. Rambeerich, D. Y. Tangman, M.R. Lollchund and M. Bhuruth, *High-order computational methods for option valuation under multifactor models*, European Journal of Operational Research 224 (2013) 219–226.

[9] C. Chiarella, B. Kang, G.H. Mayer, and A. Ziogas, The evaluation of American option prices under stochastic volatility and jump-diffusion dynamics using the method of lines, *International Journal of Theoretical and Applied Finance* 12(3)(2009)393 – 425.

[10] S. Salmi, J. Toivanen, L. Von Sydow, Iterative methods for pricing American options under the Bates model, Procedia Comput. Sci. 18 (2013) 1136-1144.

[11] J. Toivanen. A Componentwise Splitting Method for Pricing American Options Under the Bates Model. *Applied and Numerical Partial Differential Equations* 15 (2010) 213–227.

[12] D. J. Duffy, *Finite Difference Methods in Financial Engineering: a Partial Differential Approach*, John Wiley & Sons Ltd, The Atrium, Southern Gate, Chichester, West Sussex PO19 8SQ, England 2006.

[13] G. H. Golub and C. F. Van Loan, *Matrix Computations,* third edition, Johns Hopkins University Press, 1996.

[14] R. Company, L. Jódar, M. Fakharany and M.-C. Casabán. Removing the correlation term in the option pricing Heston model: numerical analysis and computing, Abstract and Applied Analysis, 2013 (2013) 1–11.

[15] M. Fakharany, R. Company, L. Jódar. Positive finite difference schemes for partial integro-differential option pricing model. *Applied Mathematics and Computation* 249 (2014) 320–332.

[16] M. Fakharany, R. Company, L. Jódar. Solving partial integro-differential option pricing problems for a wide class of infinite activity Lévy processes. *Journal of Computational and Applied Mathematics* 296 (2016) 739-752.

[17] P. R. Garabedian, *Partial Differential Equations*, AMS Chelsea Pubs. Co., 1998.

[18] M. Abramowitz, I. A. Stegun, *Handbook of mathematical functions: with formulas, graphs, and mathematical tables*, Dover Books on Mathematics 1961.

[19] R. Kangro, R. Nicolaides, Far field boundary conditions for Black–Scholes equations, SIAM Journal on Numerical Analysis 38 (4) (2000) 1357–1368.

[20] M. Ehrhardt, R. Mickens, A fast, stable and accurate numerical method for the Black–Scholes equation of american options, International Journal of Theoretical and Applied Finance 11 (2008) 471–501.

[21] J. W. Thomas, *Numerical partial differential equations: finite difference methods*, Springer, 1995.

[22] G. D. Smith, *Numerical solution of partial differential equations: finite difference methods* (3rd ed.), Clarendon Press, Oxford, UK, 1985.

[23] F. B. Hildebrand, *Introduction to numerical analysis, second edition*, Dover Publications, INC. Mineola, New York, 1987.

[24] S. Ikonen, J. Toivanen, Efficient numerical methods for pricing American options under stochastic volatility, Wiley J. Numer. Methods Partial Differ. Equ. 24 (1) (2008) 104126.

[25] S. Ikonen, J. Toivanen, Operator splitting methods for American option pricing, Appl. Math. Lett. 17 (2004) 809814.

[26] C. W. Cryer, The solution of a quadratic programming problem using systematic overrelaxation, SIAM J. Control, 9 (1971) 385–392.

[27] W. L. Briggs, V. E. Henson, S. F. McCormick, *A multigrid tutorial, second edition*, Siam, 2000.

[28] P. Wesseling, An Introduction to Multigrid Methods, John Wiley & Sons, 1992.

[29] W. Hackbusch, Multi-grid Methods and Applications, Springer, 1985.

[30] S. Salmi, J. Toivanen, L. V. Sydow, An IMEX-scheme for pricing options under stochastic volatility models with jumps, SIAM J. SCI. COMPUT., 36(2014) B817-B834.